

Core-softened water-alcohol mixtures: the solute-size effects

Murilo Sodré Marques*

*Centro das Ciências Exatas e das Tecnologias, Universidade Federal do Oeste da Bahia
Rua Bertioga, 892, Morada Nobre, CEP 47810-059, Barreiras-BA, Brazil and
Instituto de Física, Universidade Federal do Rio Grande do Sul,
Av. Bento Gonçalves 9500, Caixa Postal 15051, CEP 91501-970, Porto Alegre - RS, Brazil*

Vinícius Fonseca Hernandez and José Rafael Bordin

*Departamento de Física, Instituto de Física e Matemática,
Universidade Federal de Pelotas. Caixa Postal 354, 96001-970, Pelotas-RS, Brazil.*

(Dated: June 22, 2022)

Water is the most anomalous material on Earth, with a long list of thermodynamic, dynamic and structural behavior that deviate from the expected. Recent studies indicate that the anomalies can be related to a competition between two liquids, which means that water has a potential liquid-liquid phase transition (LLPT) that ends in a liquid-liquid critical point (LLCP). In a recent work [J. Mol. Liq. 320 (2020) 114420], using molecular dynamics simulations and a core-softened potential approach, we have shown that adding a simple solute as methanol can "kill" the anomalous behavior as the LLCP is suppressed by the spontaneous crystallization in a hexagonal closed packing (HCP) crystal near the LLPT. Now, we extend this work to see how alcohols with longer chains will affect the complex behavior of water mixtures in the supercooled regime. Besides CS methanol, ethanol and 1-propanol were added to CS water. We observed that the anomaly vanishes as the alcohol chain increases. Curiously, the LLCP did not vanishes together with the anomalous behavior. The reason is that the mechanism for ethanol and 1-propanol is distinct to the one observed previously for methanol: here, the longer chains affect the competition between the scales in the CS potential. Also, the chain size affects the solid phases, favoring the HCP solid and the amorphous solid phase over the body-centered cubic (BCC) crystal. This findings helps to elucidate the behavior of water solutions in the supercooled regime, and indicates that the LLCP can be observed in systems without anomalous behavior.

I. INTRODUCTION

Life, as we known, started and evolved in water solutions. Then, we can say that elucidate the demeanor of complex molecules in water, at both micro- and macro-levels, is of paramount importance in modern science [1, 2]. Although the behavior of complex biological proteins in water is a huge and complex problem, with many hydrophobic and hydrophilic sites, we can draw some information from simpler systems. In this way, a special class of aqueous solutions are those containing short-chain alcohols (i.e., alcohols with a small number of carbon atoms in the chain, like methanol, ethanol, or 1-propanol), most of which are miscible in water over the full range of concentrations [3, 4]. They have attracted a great attention of scientific community for decades for a number of reasons: (i) they are ubiquitous in the medical [5], food industries [6], transportation [7] and personal care [8], among others, and thus have attracted much theoretical and experimental attention; (ii) comparatively to water, the molecular structure of alcohols shows the presence of an organic radical in place of one of the hydrogen atoms; as a consequence, alcohols do not form a completely developed hydrogen-bonded network, as in the case of water; (iii) On the other hand,

the presence of both the hydroxyl group and the organic radical, usually non-polar (amphiphilic character), allows for the interaction with a huge number of organic and inorganic compounds, making alcohols good solvents, since the solute-solvent interaction can have the same order of magnitude as the solute-solute and solvent-solvent interactions [9]. In addition, (iv) although the interactions with molecules of a dual nature, such as alcohols, involve not only the hydrophobic hydration of the non-polar moiety of the molecule but also the hydrophilic interactions between the polar groups and the water molecules, still they constitute a model for the investigation of the hydrophobic effect [10, 11].

With water as a solvent, both the complexity of analysis and the richness of phenomena observed for such solutions are highlighted. Water is the most anomalous material, with more than 70 known anomalies [12]. Probably, the most well known is the density anomaly. While most of the materials increases the density upon cooling, liquid water density decreases when cooled from 4°C to 0°C at atmospheric pressure [13]. Recent findings indicated a relation between the anomalies and another unique feature of water: the liquid polymorphism and the phase transition between two distinct liquids [14]. In addition to the usual liquid-gas critical point (whose near-critical properties are so drastically different from those of liquid water [15]), since the 1990s [16] the existence of a second critical point - the liquid-liquid critical point (LLCP) has been hypothesized by simulations and subject of exten-

* murilo.sodre@ufob.edu.br

sive debate [17–21]. It has not yet been reported from experiments once is located in the so-called no-man’s land: due the spontaneous crystallization it is (almost) impossible to reach this region by experiments - however, some recent experiments show strong evidence of the existence of the LLCP [22–24]. The LLCP locates at the end of a first order liquid-liquid phase transition (LLPT) line between low-density liquid (LDL) and high-density liquid (HDL) at low temperatures [14, 16, 25–32]. Unlike the liquid–gas phase transition (LGPT), which always has a positive slope of the first-order phase transition line because $\Delta S > 0$ and $\Delta V > 0$ (Clausius–Clapeyron relation), the LLPT line can indeed be either negative or positive, depending on the pair atomic interactions of the model [33].

The critical behavior of mixtures has been widely analyzed from both an experimental and theoretical point of view [34–43]. Studies on the effects of solute size on the thermodynamic and structural properties of the aqueous solutions have been done [44–48] and, according to the authors’ knowledge, there are still no analysis of alcohol chain size influence on the critical properties and on polymorphism of these mixtures. In this way, some questions that arise are: how longer chains of alcohol will affect the behavior of CS water in the supercooled regime? How possible changes in the critical behavior can be related to the anomalous behavior? Also, there is some effect in the spontaneous crystallization observed near the LLCP?

To answer this question, we perform extensive simulations in order to analyze the phase diagram of water and water-alcohols mixtures, where both water and hydroxyls are modeled by core-softened potentials, which already have a long history of describing water anomalies both in bulk and confined environments [49–54]. In our very recent work [55] we have explored the supercooled regime of pure water, pure methanol and their mixtures using a core-softened (CS) potential model [2]. In this scheme, hydroxyl groups of different molecules interact by a continuous shouldered well (CSW) potential, while all other interactions are reproduced by LJ-like contributions, and our principal focus in that publication was on the relations between density anomaly, liquid-liquid phase transition and spontaneous crystallization by means of Molecular Dynamics simulations. In the present work, in a similar way to that performed by Urbic et al [56], we extend this scheme to ethanol (CH_3-CH_2-OH) and 1-propanol ($CH_3-CH_2-CH_2-OH$), by modeling such alcohols as linear chains constituted by three (trimers) and four (tetramers) partially fused spheres, respectively, and the primary objective is to complement our previous study by exploring the influence of the size of the solute on the thermodynamic properties of mixtures of core-softened water and alcohols: methanol, ethanol and 1-propanol.

The remaining of the paper is organized as follows. In Section II we present our interaction models for water and alcohols molecules, and summarize the details of the simulations. Next, in section III our most significant results for our CS mixture model are introduced. In par-

ticular, we will focus on the concentration dependence of the LLCP and influence on the excess entropy of mixture in comparison with pure CS water. The paper is closed with a brief summary of our main conclusions and perspectives.

II. MODEL AND SIMULATION DETAILS

Our water-like solvent here will be modeled by a 1-site core-softened fluid in which particles interact with the potential model proposed by Franzese [57]. Water-like particles W_{CS} are represented by spheres with a hard-core of diameter a and a soft-shell with radius $2a$, whose interaction potential is given by

$$U^{CS}(r) = \frac{U_R}{1 + \exp[\Delta(r - R_R)]} - U_A \exp\left(-\frac{(r - R_A)^2}{2\delta_A^2}\right) + U_A \left(\frac{a}{r}\right)^{24}. \quad (1)$$

With the parameters $U_R/U_A = 2$, $R_R/a = 1.6$, $R_A/a = 2$, $(\delta_A/a)^2 = 0.1$, and $\Delta = 15$ this potential displays an attractive well for $r \sim 2a$ and a repulsive shoulder at $r \sim a$, as can be seen in figure 1(a) (red curve). The competition between these two length scales leads to water-like anomalies, as the density, diffusion anomalies, and to the existence of a liquid liquid critical point [57–60].

As a direct extension and building on our previous work on mixtures of water and methanol, where a single methanol molecule was constituted by two tangent spheres, in this work we have followed the extension made by Urbic et al towards ethanol (CH_3-CH_2-OH) and 1-propanol ($CH_3-CH_2-CH_2-OH$) being modeled as linear trimers and tetramers, respectively (Fig. 1). Trimers are constructed as linear rigid molecules consisting of three partially fused spheres, where two adjacent spheres are placed at fixed distance $L_{ij} = 0.60a$, with a as the unit length. Analogously, tetramers are modeled as linear rigid molecules consisting of four partially fused spheres, where two adjacent spheres are placed at fixed distance $L_{ij} = 0.78a$. In all models, hydroxyl groups interact through a soft-core potential (eq 1), while CH_2 and CH_3 groups are nonpolar and interact through LJ-like potential,

$$U^{LJ} = \frac{4}{3} 2^{2/3} \epsilon \left[\left(\frac{\sigma}{r}\right)^{24} - \left(\frac{\sigma}{r}\right)^6 \right], \quad (2)$$

$OH-CH_2$ and $OH-CH_3$ interactions are of LJ type as well. LJ parameters are reported in Table I. As in last work, quantities are reported in reduced dimensionless units relative to the hydroxyl group diameter and the depth of its attractive well.

The simulations were performed in the NPT ensemble with a fixed number of molecules ($N_{tot} = 1000$). $N_{alc} = x_{alc}N_{tot}$ is the number of alcohol (methanol, ethanol or propanol) molecules and $N_w = N_{tot} - N_{alc}$

	L_{ij}	ϵ_{1n}	ϵ_{nn}	σ_{1n}	σ_{nn}
Dimers	1.000	0.316	0.100	1.000	1.000
Trimers	0.600	0.400	0.400	1.115	1.230
Tetramers	0.780	0.500	0.500	1.115	1.230

TABLE I. Potential parameters for dimers ($n = 2$), trimers ($n = 2, 3$), and tetramers ($n = 2, 3, 4$); the OH group is labeled with 1. As for the bond length, $j = i + 1$ [56].

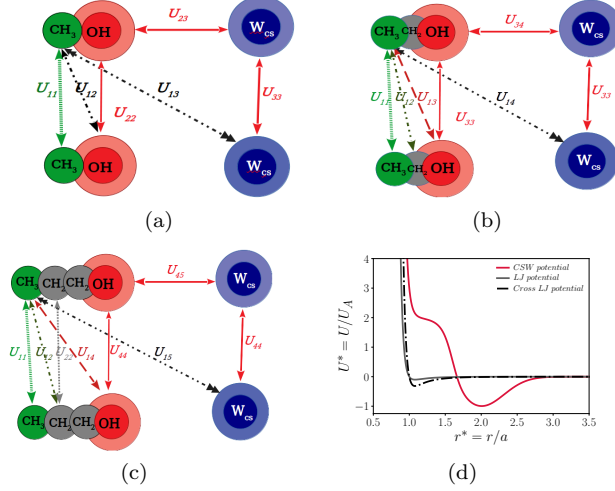


FIG. 1. In (a), (b) and (c), our model for methanol, ethanol and 1-propanol is outlined, while in (d) we see the interaction between water and hydroxyl's is described by the CSW potential, while other interactions behave like a 24-6 Lennard-Jones potential.

that of water molecules, where x_{alc} is the alcohol mole fraction, which has been varied from 0.0 (pure water), 0.01, 0.05 and 0.1 (we've focused in low-concentration range). The temperature and pressure were controlled using the optimized constant pressure stochastic dynamics proposed by Kolb and Dünweg [61] as implemented in the ESPResSo package [62, 63]. This barostat implementation allows for the use of a large time step. This was set to $\delta t^* = 0.01$, and the equations of motion were integrated using the velocity Verlet algorithm. The Langevin thermostat [64], that keeps the temperature fixed, has a coupling parameter $\gamma_0 = 1.0$. The piston parameters for the barostat are $\gamma_p = 0.0002$ and mass $m_p = 0.001$. The particles were randomly placed in a cubic box, and then dynamics was run for 5×10^6 time steps in the NVT ensemble to thermalize the system. This was followed by 1×10^6 time steps in the NPT ensemble to equilibrate the system's pressure and 1×10^7 time steps further for the production of the results, with averages and snapshots being taken at every 1×10^5 steps. To ensure that the system temperature and pressure were well controlled we averaged this quantities during the simulations. As well, to monitor the equilibration the evolution of the potential energy along the simulation was followed. Here, the molecule density ρ is defined as $N_m / \langle V_m \rangle$ with $\langle V_m \rangle$ being the mean volume at a given pressure and

temperature. Isotherms were evaluated from $T^* = 0.20$ up to $T^* = 0.70$ with changing intervals - a finer grid was used in the vicinity of the critical points. In the same sense, the pressure was varied from $P = 0.005$ up to $P = 0.30$ with distinct intervals.

Also in a similar way to the previous work, we evaluated the temperature of maximum density (TMD) and the locus of the maximum of response functions close to the critical point at the fluid phase (the isothermal compressibility κ_T , the isobaric expansion coefficient α_P and the specific heat at constant pressure C_P):

$$\kappa_T = \frac{1}{\rho} \left(\frac{\partial \rho}{\partial P} \right)_T, \alpha_P = -\frac{1}{\rho} \left(\frac{\partial \rho}{\partial T} \right)_P, C_P = \frac{1}{N_{tot}} \left(\frac{\partial H}{\partial T} \right)_P, \quad (3)$$

where $H = U + PV$ is the system enthalpy, with V the mean volume obtained from the NPT simulations. The quantities shown in the Electronic Supplementary Material (ESI)[†] were obtained by numerical differentiation. As consistency check, we have obtained the same maxima locations when using statistical fluctuations: the compressibility is a measure of volume fluctuations, the isobaric heat capacity is proportional to the entropy fluctuations experienced by N molecules at fixed pressure, and the thermal expansion coefficient reflects the correlations between entropy and volume fluctuations [64, 65].

In order to describe the connection between structure and thermodynamics, we have analyzed the radial distribution function (RDF) $g(r^*)$, which was subsequently used to compute the excess entropy. s_{ex} can be obtained by counting all accessible configurations for a real fluid and comparing with the ideal gas entropy [66]. Consequently, the excess entropy is a negative quantity since the liquid is more ordered than the ideal gas. Note that s_{ex} increases with temperature just like the full entropy S does; in fact $s_{ex} \rightarrow 0$ as temperature goes to infinity at fixed density because the system approaches to an ideal gas [67, 68]. Analytically, the excess entropy may be computed if the equation of state is known [69]. A systematic expansion of s_{ex} exists in terms of two-particle, three-particle contributions, etc.,

$$s_{ex} = s_2 + s_3 + s_4 + \dots \quad (4)$$

The two-particle contribution is calculated from the radial distribution function $g(r)$ as follows:

$$s_2 = -2\pi\rho \int_0^\infty [g(r)\ln g(r) - g(r) + 1] r^2 dr, \quad (5)$$

since s_2 is the dominant contribution to excess entropy [70, 71] and it is proved to be between 85% and 95% of the total excess entropy in Lennard-Jones systems [72]. Also, the translational order parameter τ was evaluated. It is defined as [73]

$$\tau \equiv \int_0^{\xi_c} |g(\xi) - 1| d\xi, \quad (6)$$

where $\xi = r\rho^{1/2}$ is the interparticle distance r scaled with the average separation between pairs of particles $\rho^{1/2}$. ξ_c is a cutoff distance, defined as $\xi_c = L\rho^{1/2}/2$, where L is the simulation box size. For an ideal gas (completely uncorrelated fluid), $g(\xi) = 1$ and τ vanishes. For crystal or fluids with long range correlations $g(\xi) \neq 1$ over long distances, which leads to $\tau > 0$. The excess entropy and the translational order parameter τ are linked once both are dependent on the deviation of $g(r)$ from unity.

Another structural quantity evaluated was the orientational order parameter (OOP), that gives insight on the local order [73–76]. The OOP for a specific particle i with N_b neighbors, is given by

$$q_l(i) = \sqrt{\frac{4\pi}{2l+1} \sum_{m=-l}^l |q_{lm}|^2}, \quad (7)$$

with

$$q_{lm}(i) = \sqrt{\frac{1}{N_b} \sum_{j=1}^{N_b} Y_{lm}(\theta(\vec{r}_{ij}), \phi(\vec{r}_{ij}))}. \quad (8)$$

where Y_{lm} are the spherical harmonics of order l and \vec{r}_{ij} is the vector from particle i to its neighbour j . The OOP for a whole system is obtained taking the average over the parameter value for each particle i , $q_l = \langle q_l(i) \rangle_i$. In this work we evaluated the OOP for $l = 6$, using the freud python library [77], and the number of neighbors for each particle was found computing Voronoi diagrams using voro++ [78].

The dynamic behaviour was analyzed by the mean square displacement (MSD), given by

$$\langle [\vec{r}(t) - \vec{r}(t_0)]^2 \rangle = \langle \Delta \vec{r}(t)^2 \rangle, \quad (9)$$

where $\vec{r}(t_0)$ and $\vec{r}(t)$ denote the particle position at a time t_0 and at a later time t , respectively. The MSD is then related to the diffusion coefficient D by the Einstein relation,

$$D = \lim_{t \rightarrow \infty} \frac{\langle \Delta \vec{r}(t)^2 \rangle}{6t}. \quad (10)$$

For alcohol molecules we have considered the center of mass displacement. The onset of crystallization was monitored analyzing the local structural environment of particles by means of the Polyhedral Template Matching (PTM) method implemented in the Ovito software [79, 80]. Ovito was also employed to visualize the phases and take the system snapshots.

III. RESULTS AND DISCUSSION

A. Pure CS Water phase diagram

Water is fascinating and unique. From its numerous anomalous behaviors the most well known is, probably,

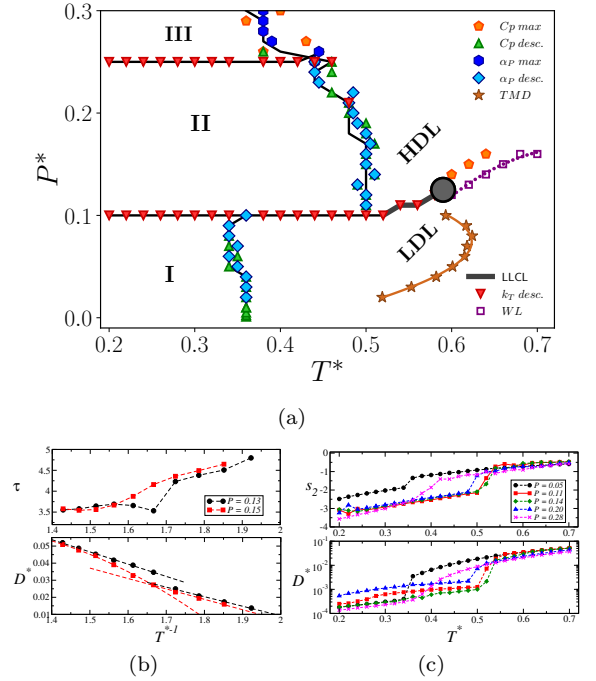


FIG. 2. (a) PT phase diagrams for pure CS water showing the solid phases I (BCC solid), II (HCP solid) and III (amorphous solid) and the low and high density liquid phases. The points in the phase separations indicate distinct discontinuities or maxima in the evaluated response functions. The Widom Line corresponds to maxima in κ_T . The solid-liquid coexistence lines were drawn based in the discontinuities in the pair excess entropy, the structure factor (not shown here for simplicity) and in the diffusion constant, as indicated in the figure (b). Also, the pair excess entropy (not shown here for simplicity), the structure factor and D^* have discontinuities in the LDL-HDL transition, as we show in the figure (c) for the subcritical isobar $P^* = 0.13$, and a fragile to strong transition for the supercritical isobar $P^* = 0.15$ as it crosses the Widom Line.

the density anomaly. It be characterized by the Temperature of Maximum Density (TMD) line, that corresponds to the maxima in the $\rho \times T$ isobar. Recent findings indicates that the water anomalies are related to the Liquid-Liquid Critical Point (LLCP) [16, 81]. Although hypothetical and not observed (yet) in experiments, there is strong and many evidences that the water liquid polymorphism in the supercooled regime ends in the LLCP [14, 82]. We can estimate the critical point location using the isothermal density derivatives of the pressure [83]

$$\left(\frac{\partial P}{\partial \rho} \right)_T = \left(\frac{\partial^2 P}{\partial \rho^2} \right)_T = 0. \quad (11)$$

Coming from the supercritical region, the LLCP lays at the end of the Widom Line (WL) - a line in the $P \times T$ phase diagram that can be obtained by the maxima in the response function κ_T and corresponds to the separation between LDL-like and HDL-like behavior in the

supercritical regime. In the figure 2 (a) we show the CS water phase diagram obtained from our simulations. The WL, indicated by the dotted purple line and the purple squares, ends at the LLCP. Below the LLCP we have the transition between the liquid phases, indicated by the discontinuity in the thermodynamic property κ_T – shown in the ESI[†] for all isotherms – and in the structural and dynamic properties. For instance, the upper panel in the figure 2(b) shows the structure factor τ for the subcritical pressure $P^* = 0.13$ and for the supercritical pressure $P^* = 0.15$ as function of the inverse of temperature. As T decreases we can see a discontinuity in the subcritical isobar, indicating an abrupt change in the fluid structure. On the other hand, the supercritical isobar has a monotonic increase in τ as T decreases, indicating an increase in the particles order. Similarly, the dependence of the diffusion coefficient D with T^{*-1} is discontinuous in the supercritical isobar. For the supercritical pressure $P^* = 0.15$ we see a change in the diffusion inclination with temperature when it crosses the Widom Line, indicating the HDL-dominated to LDL-dominated regime. These results are in agreement with our recent work obtained by the heating of the system [55] and previous works employing this potential [57–60].

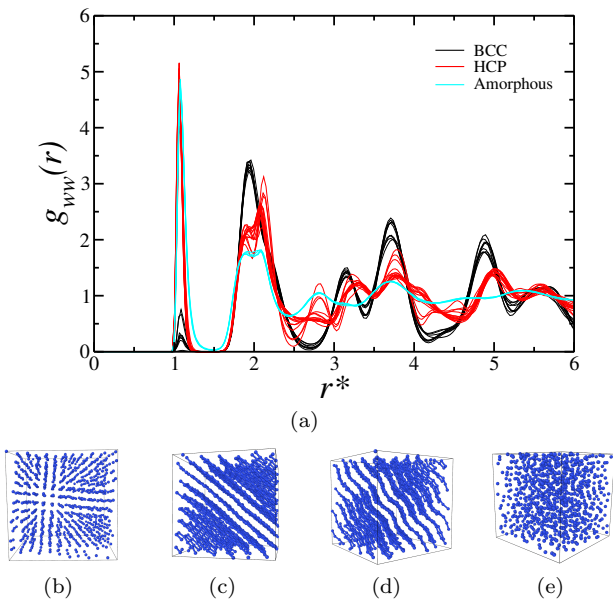


FIG. 3. (a) CS water-water radial distribution function (RDF) along the isotherm $T^* = 0.26$. Black lines are the pressures in the BCC phase, red lines in the HCP phase and cyan in the amorphous phase. System snapshots in the (b) BCC phase, HCP phase with (c) straight or (d) rippled planes and in (e) the amorphous solid phase.

However, the solid phases weren't explored for this system. In fact, the HCP phase was observed in our work [55] and in the study by Hus and Urbic using the methanol model [84, 85]. Here, exploring a larger region in the phase diagram, we characterized three distinct solid phases. The solid phase I corresponds to a body-

centered cubic (BCC) crystal at lower pressures. Increasing P it changes to the solid phase II, with a hexagonal closed packed (HCP) structure, and at even higher compression we observe the amorphous solid, named phase III. The transition between the solid phases, and from LDL to HCP, are well defined by the discontinuous behavior in κ_T , shown in the SI. The transition from solid phase I to LDL and from solid phase II to HDL have discontinuities in the response functions α_p and C_p , shown in the SI. Also, the structure (here characterized by the pair excess entropy) and the dynamic behavior (given by the diffusion coefficient) are discontinuous for these solid-fluid transition. This can be observed in the figure 2(c). Here, the pressure $P^* = 0.05$ is a isobar that cross the BCC-LDL transition, $P^* = 0.11, 0.14$ and 0.20 the HCP-HDL transition and $P^* = 0.28$ the amorphous-HDL transition. As we can see, the structure and dynamics change smoothly for this last transition, as the magenta line for $P^* = 0.28$ indicates in the figure 2 (c). Also, the response functions C_p and α_p are not discontinuous in this transition, but have a maximum – indicating that this is a second order, smooth transition. The distinct phases can also be observed when we analyze the water-water radial distribution function (RDF) $g_{ww}(r)$ along one isotherm. For instance, we show in the figure 3(a) the $g_{ww}(r)$ for pressures ranging from $P^* = 0.01$ to $P^* = 0.30$ along the isotherm $T^* = 0.26$. We can see clear changes in the structure as P varies. At lower pressures the particles are separated mainly at the second length scale, characterizing the BCC phase – a snapshot at $P^* = 0.01$ and $T = 0.26$ is shown in the figure 3(b). Increasing the pressure the system changes for the HCP phase, where the occupation in the first length scale dominates the structure. In fact, the HCP planes are separated by a distance equal to the second length scale, while the distance between particles in the same plane is the first length scale. It becomes clear when we use the Ovito [80] feature "create bonds" if the distance is equal to the first scale. While for the BCC snapshot we did not see any bond, for the HCP snapshot at $P^* = 0.14$ in the figure 3(c) we can see the bonds between particles in the same plane. As P grows, the HCP planes get rippled, as we can see in figure 3(d) for $P^* = 0.24$ and in the behavior of the RDF red lines. Finally, it changes to an amorphous structure at high pressure, as we show for $P^* = 0.30$ in figure 3(e).

Now, with the phase behavior of the CS water model depicted, we can see how the presence of short alcohol affects the observed phases and the density anomaly.

B. Water-short alcohol mixtures

Small concentrations of short chain alcohols such as methanol, ethanol and 1-propanol create a very interesting effect in the TMD line [86, 87]. They act as "structure maker", promoting the low density ice-like water structure and increasing the TMD. This is usually observed for alcohol concentrations χ_{alc} smaller than 0.01 - and is not

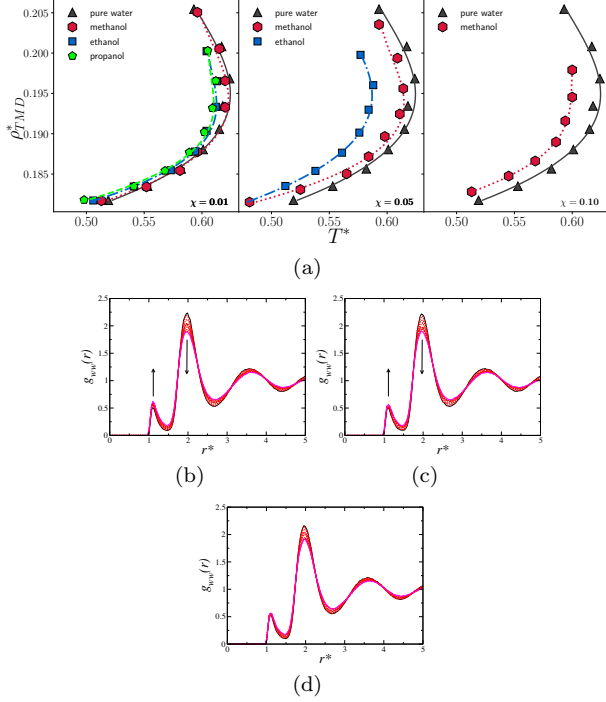


FIG. 4. (a) TMD behaviour of all CS alcohols used in this work: for $\chi_{alc} = 0.05$, 1-propanol didn't show TMD and for $\chi_{alc} = 0.10$, only methanol shows TMD. (b) CSW-CSW radial distribution function $g_{ww}(r)$ along the isobar $P^* = 0.08$ for water-ethanol at $\chi_{alc} = 0.10$ case with temperatures ranging from $T = 0.50$ (black solid line) to $T = 0.68$ (magenta solid line). The intermediate temperatures are shown with red dashed lines. The arrows indicate the competition between the scales as T increases. (c) is for the case with ethanol concentration at $\chi_{alc} = 0.05$, were the competition between the scales and the TMD are still observable, while for (d) $\chi_{alc} = 0.10$ both competition and TMD vanish.

our goal here. We want to analyze the TMD vanishing and what happens in the phase diagram as it vanishes. This can be observed as x increases and methanol acts as "structure breaker". Using the CS model for water-methanol mixtures [55] we found that the TMD persists up to high methanol concentrations, as $\chi < 70\%$ – much higher than in experiments. This is a consequence of the model: the same potential is employed for water-water, water-OH and OH-OH. On the other hand, the energy for the water-water h-bonds is equal to the water-OH h-bonds. Nevertheless, we can increase the structure breaker effect by increasing the solute size. In fact, for ethanol the TMD line vanishes at $\chi_{alc} = 0.10$, while for 1-propanol the TMD is only observed at $\chi_{alc} = 0.01$ – the TMD lines are shown in the figure 4(a).

The water anomalous behavior is related to the competition between two liquids that coexist [14, 88, 89]. This competition can be observed using the $g_{ww}(r)$. Here we show the RDFs the isobar $P^* = 0.080$ between the temperatures $T^* = 0.50$ and $T^* = 0.68$ for a fraction of ethanol of $\chi_{alc} = 0.01$ in the figure 4(b), for $\chi_{alc} = 0.05$

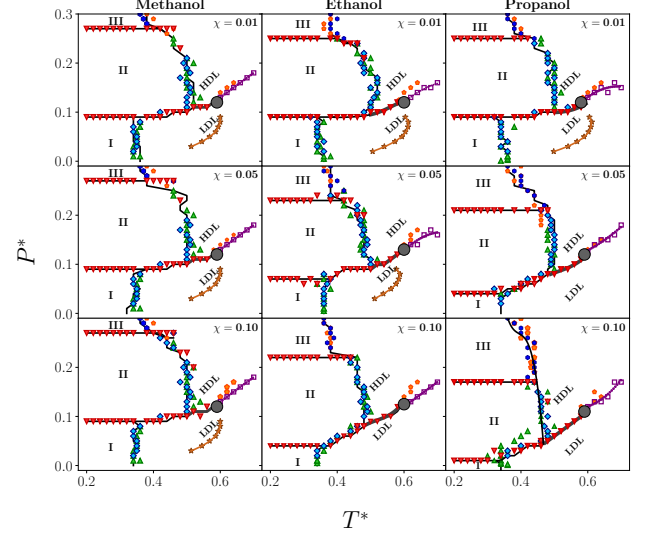


FIG. 5. PT phase diagrams for aqueous solutions of (a) methanol, (b) ethanol and (c) propanol for all concentrations analyzed in this work.

in the figure 4(c) and for $\chi_{alc} = 0.10$ in figure 4(d). As we can see, for the fractions $\chi_{alc} = 0.01$ and $\chi_{alc} = 0.05$ we observe the competition between the scales: the water particles migrates from the second length scale to the first length scale as T increases, as indicated by the arrows. On the other hand, for $\chi_{alc} = 0.10$ there is practically no increase in the occupation of the first length scale as the occupation in the second length scale decreases. Once there is no competition, we do not observe the density anomaly. This indicates that adding higher concentration of alcohol changes the competition between the scales in the CSW water model and that the CS alcohol chain length also affects the competition – in our previous work for methanol, we only observe this at $\chi_{alc} = 0.70$ [55].

Curiously, even without the density anomaly, all the water-alcohol mixtures have liquid-liquid phase transition. In the figure 5 we show the PT phase diagrams for all the fractions and types of alcohols. After the liquid-liquid critical point, The Widom Line (WL) separates water with more HDL-like local structures at high temperatures from water with more LDL-like local structures at low temperatures [90]. Looking at the diffusion coefficient D^* isotherms we can see the distinct transitions. At lower temperatures, as $T^* = 0.34$ it melts from the solid phase to the HDL phase at high pressures, as we show in the figure 6. Increasing T^* , we can see the system going from the LDL phase (with $D^* > 0$) to the HCP phase, with diffusion near zero, to the HDL phase, where D^* increases again. In the isotherms that cross the LDL-HDL transition we can see the discontinuity in the curve, indicating the phase transition. Above the LLCP we can see a change in the $D^* \times P^*$ curve behavior as it

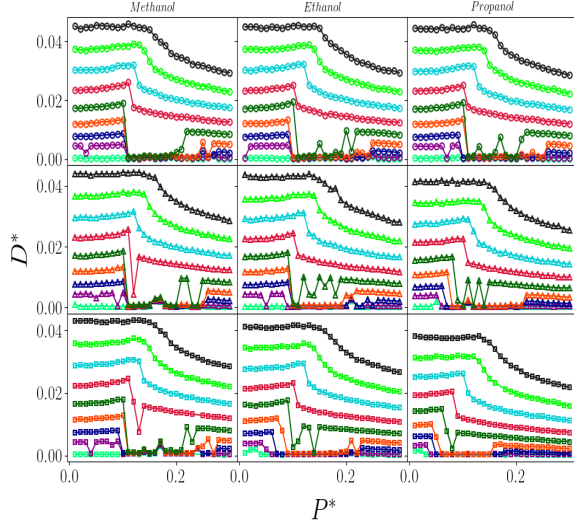


FIG. 6. Diffusion coefficient versus pressure for all solutions analyzed in this work. From bottom to top in each diagram, we have the isotherms $T^* = 0.34, 0.38, 0.42, \dots, 0.66$. Each row represents a concentration of solute: $x_{alc} = 0.01, 0.05$ and 0.1

crosses the WL.

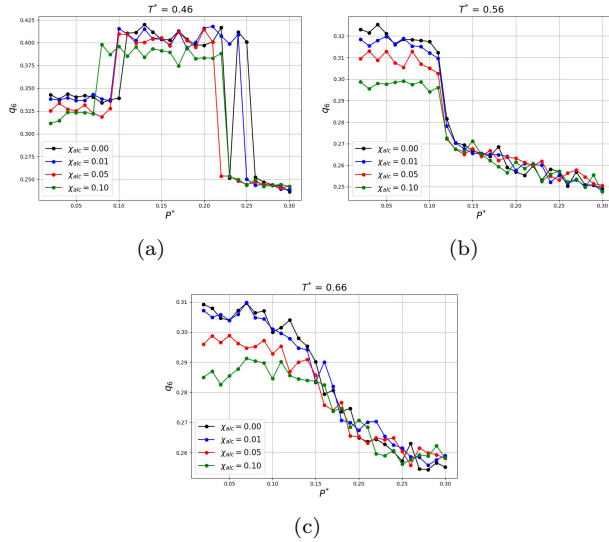


FIG. 7. Local bond orientation order parameter q_6 as function of pressure for the isotherms (a) $T^* = 0.46$, (b) $T^* = 0.56$ and (c) $T^* = 0.66$.

The same discontinuity can be observed in the structural behavior. Besides τ and s_2 , we also evaluated the q_6 to analyze the structure. For simplicity, we show here only the case of pure water and water-ethanol mixtures. Along the isotherm $T^* = 0.46$, that crosses the phases LDL, HCP and HDL, we can see in the figure 7(a) clearly the discontinuities corresponds to this transitions for all fractions of ethanol. Also, it is noticeable how the

ethanol is structure breaker: the value of q_6 in the LDL and HCP phases are smaller as χ_{alc} increases. Along the isotherm $T^* = 0.56$, shown in the figure 7(b), we can see the same structure breaker effect in the LDL regime, and a discontinuous transition to the HDL phase. In contrast, above the LLCP there is no discontinuity. The isotherm $T^* = 0.66$, shown in the figure 7(c), have a smooth decay in q_6 as it crosses the WL and goes from LDL-like to HDL-like. This is interesting, once it indicates that a system can have a LLCP without have density anomaly.

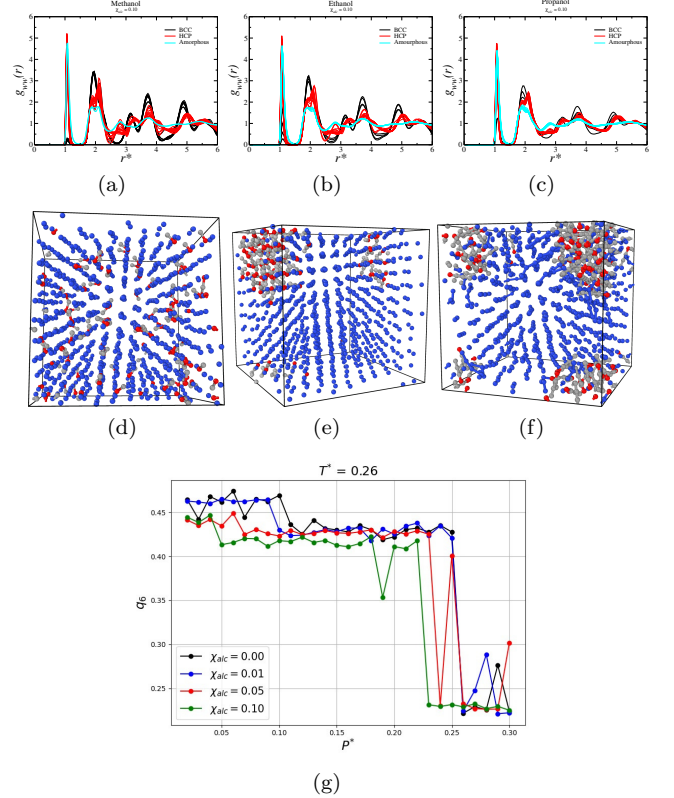


FIG. 8. CSW-CSW radial distribution function $g_{ww}(r)$ along the isotherm $T^* = 0.26$ for water-alcohol mixtures with $\chi_{alc} = 0.10$ for (a) methanol, (b) ethanol and (c) propanol. Snapshots for the correspondents mixtures: $\chi_{alc} = 0.10$ of (d) methanol, (e) ethanol and (f) propanol. (g) Local bond orientation order parameter q_6 as function of pressure for the isotherm $T^* = 0.26$.

As in the pure CSW water case, three solid phases were observed. However, an interesting finding is how the carbon chain length affects the solid phases. It is clear that longer apolar chains affects the extension of the region occupied by each solid phase: the BCC crystal (region I) loses space, moving to lowers pressures. Likewise, the HCP crystal (region II) moves to lower pressures as the alcohol chain increase. However, the area occupied in the PT phase diagram remains - it just shifts to lower pressures as the size and fraction of alcohol increases. For this two solid phases, the temperature range in the PT phase diagram seems to be independent of the fraction χ_{alc} . On the other hand, the amorphous solid phase (region III)

is favored as the it expands its extension to lower pressures and higher temperatures as the apolar chain grows. To understand why the HCP phase remains occupying a large area in the phase diagram while the BCC area shrinks we show in the figure 8 the $g_{ww}(r)$ for the three alcohols with fraction $\chi_{alc} = 0.10$ along the isotherm $T^* = 0.26$ from $P^* = 0.01$ to $P^* = 0.30$. Comparing the three cases with the pure CSW case, figure 3(a), is clear that increasing the size of the apolar tail in the alcohol favor the occupation in the second length scale. While for methanol and ethanol we see a low occupation in the first length scale at the lower pressures, for propanol this occupancy is high even for $P^* = 0.01$. This is consequence of a alcohol bubble formation: for the CS methanol, once the molecule size is comparable to the second length scale and the OH is modeled as a CSW particle, the molecules merge in the BCC structure, as we show in the figure 8(d). However, the longer alcohols creates bubbles, as we can see in figure 8(e) and (f) for ethanol and propanol, respectively. It alters the water structure near the bubbles, favoring the first length scale. It reflects in the local orientation. In the figure 8(g) we show the q_6 for this isotherm for the case of pure CS water ($\chi_{alc} = 0.00$) and the three fractions of ethanol. We can see that for both crystal phases, BCC and HCP, the local order is affected by the alcohol once q_6 is small for higher fractions.

IV. CONCLUSIONS

In this paper we have explored the supercooled regime of pure water and mixtures of water and short chain alcohols: methanol, ethanol and propanol using a two-length scale core-softened potential approach. Our aim has been to understand the influence of chain size on den-

sity anomaly, the liquid-liquid phase transition and on the polymorphism which are generally observed in these models. There's a pronounced influence of the apolar chain size on solid polymorphism. The BCC phase loses space in the phase diagram once longer alcohols favor the occupancy in the first length scale. Once the HCP phase has a higher occupancy in this length scale it is shifted to smaller pressures, while the amorphous solid phase grows favored by the disorder induced by alcohol.

The density anomaly vanishes as the competition between the scales is suppressed in the LDL phase. However, the LDL-HDL phase transition persists for all cases. This indicates that the competition between two liquids is connected with waterlike anomalies, but the system will no necessarily have the anomalies if it has a liquid-liquid phase transition and liquid-liquid critical point. This results helps to understand the complex behavior of water and mixtures with amphiphilic solutes in the supercooled regime.

ACKNOWLEDGMENTS

MSM thanks the Brazilian Agencies Conselho Nacional de Desenvolvimento Científico e Tecnológico (CNPq) for the PhD Scholarship and Coordenação de Aperfeiçoamento de Pessoal de Nível Superior (CAPES) for the support to the collaborative period in the Instituto de Química Física Rocasolano. VFH thanks the CAPES, Finance Code 001, for the MSc Scholarship. JRB acknowledge the Brazilian agencies CNPq and Fundação de Apoio a Pesquisa do Rio Grande do Sul (FAPERGS) for financial support. All simulations were performed in the SATOLEP Cluster from the Group of Theory and Simulation in Complex Systems from UFPel.

V. REFERENCES

-
- [1] J. Rowlinson and F. Swinton, *Liquids and Liquid Mixtures*, Butterworths monographs in chemistry and chemical engineering (Butterworth Scientific, 1982).
 - [2] G. Franzese and M. Rubi, *Aspects of Physical Biology: Biological Water, Protein Solutions, Transport and Replication*, Lecture Notes in Physics (Springer Berlin Heidelberg, 2008).
 - [3] Y. Koga, *Solution Thermodynamics and its Application to Aqueous Solutions: A Differential Approach* (Elsevier Science, 2007).
 - [4] E. Ruckenstein and I. Shulgin, *Thermodynamics of Solutions: From Gases to Pharmaceuticals to Proteins*, SpringerLink: Springer e-Books (Springer New York, 2009).
 - [5] N. K. Hermkens, R. L. Aspers, M. C. Feiters, F. P. Rutjes, and M. Tessari, Trace analysis in water-alcohol mixtures by continuous p-h2 hyperpolarization at high magnetic field, *Magnetic Resonance in Chemistry* **56**, 633 (2018).
 - [6] T. V. N. Nguyen, L. Paugam, P. Rabiller, and M. Rabiller-Baudry, Study of transfer of alcohol (methanol, ethanol, isopropanol) during nanofiltration in water/alcohol mixtures, *Journal of Membrane Science* **601**, 117907 (2020).
 - [7] P. Prslja, E. Lomba, P. Gómez-Álvarez, T. Urbic, and E. G. Noya, Adsorption of water, methanol, and their mixtures in slit graphite pores, *The Journal of Chemical Physics* **150**, 024705 (2019), <https://doi.org/10.1063/1.5078603>.
 - [8] L. M. Vane, Review: membrane materials for the removal of water from industrial solvents by pervaporation and vapor permeation, *Journal of Chemical Technology & Biotechnology* **94**, 343 (2019).
 - [9] F. Franks, R. S. of Chemistry (Great Britain), and R. S. of Chemistry (Great Britain)., *Water: A Matrix of Life*, RSC paperbacks (Royal Society of Chemistry, 2000).

- [10] N. T. Southall, K. A. Dill, and A. D. J. Haymet, A view of the hydrophobic effect, *The Journal of Physical Chemistry B* **106**, 521 (2002), <https://doi.org/10.1021/jp015514e>.
- [11] E. Xi and A. J. Patel, The hydrophobic effect, and fluctuations: The long and the short of it, *Proceedings of the National Academy of Sciences* **113**, 4549 (2016), <https://www.pnas.org/content/113/17/4549.full.pdf>.
- [12] M. Chaplin, Anomalous properties of water, <http://www.lsbu.ac.uk/water/anmlies.html> (2020).
- [13] G. S. Kell, Density, thermal expansivity, and compressibility of liquid water from 0.deg. to 150.deg., correlations and tables for atmospheric pressure and saturation reviewed and expressed on 1968 temperature scale., *J. Chem. Eng. Data* **20**, 97 (1975).
- [14] P. Gallo, K. Amann-Winkel, C. A. Angell, M. A. Anisimov, F. Caupin, C. Chakravarty, E. Lascaris, T. Loerting, A. Z. Panagiotopoulos, J. Russo, J. A. Sellberg, H. E. Stanley, H. Tanaka, C. Vega, L. Xu, and L. G. M. Pettersson, Water: A tale of two liquids, *Chemical Reviews* **116**, 7463 (2016), pMID: 27380438, <https://doi.org/10.1021/acs.chemrev.5b00750>.
- [15] M. A. Anisimov, J. V. Sengers, and J. M. Levelt Sengers, Chapter 2 - near-critical behavior of aqueous systems, in *Aqueous Systems at Elevated Temperatures and Pressures*, edited by D. A. Palmer, R. Fernández-Prini, and A. H. Harvey (Academic Press, London, 2004) pp. 29–71.
- [16] P. Poole, F. Sciortino, U. Essmann, and H. Stanley, Phase-behavior of metastable water, *Nature* **360**, 324 (1992).
- [17] D. T. Limmer and D. Chandler, The putative liquid-liquid transition is a liquid-solid transition in atomistic models of water, *The Journal of Chemical Physics* **135**, 134503 (2011), <https://doi.org/10.1063/1.3643333>.
- [18] D. T. Limmer and D. Chandler, The putative liquid-liquid transition is a liquid-solid transition in atomistic models of water. ii, *The Journal of Chemical Physics* **138**, 214504 (2013), <https://doi.org/10.1063/1.4807479>.
- [19] P. H. Poole, R. K. Bowles, I. Saika-Voivod, and F. Sciortino, Free energy surface of st2 water near the liquid-liquid phase transition, *The Journal of Chemical Physics* **138**, 034505 (2013), <https://doi.org/10.1063/1.4775738>.
- [20] J. C. Palmer, R. Car, and P. G. Debenedetti, The liquid-liquid transition in supercooled st2 water: a comparison between umbrella sampling and well-tempered metadynamics, *Faraday Discuss.* **167**, 77 (2013).
- [21] J. C. Palmer, A. Haji-Akbari, R. S. Singh, F. Martelli, R. Car, A. Z. Panagiotopoulos, and P. G. Debenedetti, Comment on “the putative liquid-liquid transition is a liquid-solid transition in atomistic models of water” [i and ii: *J. chem. phys.* 135, 134503 (2011); *j. chem. phys.* 138, 214504 (2013)], *The Journal of Chemical Physics* **148**, 137101 (2018), <https://doi.org/10.1063/1.5029463>.
- [22] F. Caupin, Escaping the no man’s land: Recent experiments on metastable liquid water, *Journal of Non-Crystalline Solids* **407**, 441 (2015), 7th IDMRCS: Relaxation in Complex Systems.
- [23] A. Taschin, P. Bartolini, R. Eramo, R. Righini, and R. Torre, Evidence of two distinct local structures of water from ambient to supercooled conditions, *Nat. Comm.* **4**, 2401 (2013).
- [24] N. J. Hestand and J. L. Skinner, Perspective: Crossing the widom line in no man’s land: Experiments, simulations, and the location of the liquid-liquid critical point in supercooled water, *The Journal of Chemical Physics* **149**, 140901 (2018), <https://doi.org/10.1063/1.5046687>.
- [25] H. Stanley, L. Cruz, S. Harrington, P. Poole, S. Sastry, F. Sciortino, F. Starr, and R. Zhang, Cooperative molecular motions in water: The liquid-liquid critical point hypothesis, *Physica A: Statistical Mechanics and its Applications* **236**, 19 (1997), proceedings of the Workshop on Current Problems in Complex Fluids.
- [26] O. Mishima and H. Stanley, The relationship between liquid, supercooled and glassy water, *Nature* **396** (1998).
- [27] H. Stanley, S. Buldyrev, O. Mishima, M. Sadr-Lahijany, A. Scala, and F. Starr, Unsolved mysteries of water in its liquid and glassy phases, *Journal of Physics: Condensed Matter* **12**, A403 (2000).
- [28] F. Sciortino, E. la Nave, and P. Tartaglia, Physics of the liquid-liquid critical point, *Physical review letters* **91**, 155701 (2003).
- [29] P. G. Debenedetti, Supercooled and glassy water, *Journal of Physics: Condensed Matter* **15**, R1669 (2003).
- [30] P. Debenedetti and H. Stanley, Supercooled and glassy water, *Physics Today* **56**, 40 (2003).
- [31] H. Eugene Stanley, Liquid and glassy water: Two materials of interdisciplinary interest, in *Handbook of Materials Modeling: Methods*, edited by S. Yip (Springer Netherlands, Dordrecht, 2005) pp. 2917–2922.
- [32] P. H. Handle, T. Loerting, and F. Sciortino, Supercooled and glassy water: Metastable liquid(s), amorphous solid(s), and a no-man’s land, *Proceedings of the National Academy of Sciences* **114**, 13336 (2017), <https://www.pnas.org/content/114/51/13336.full.pdf>.
- [33] H. M. Gibson and N. B. Wilding, Metastable liquid-liquid coexistence and density anomalies in a core-softened fluid, *Phys. Rev. E* **73**, 061507 (2006).
- [34] J. C. Forman and G. Thodos, Experimental determination of critical temperatures and pressures of mixtures: The methane-ethane-n-butane system, *AIChE Journal* **8**, 209 (1962).
- [35] F. H. Stillinger and E. Helfand, Critical solution behavior in a binary mixture of gaussian molecules, *The Journal of Chemical Physics* **41**, 2495 (1964), <https://doi.org/10.1063/1.1726293>.
- [36] J. Levelt Sengers, G. Morrison, and R. Chang, Critical behavior in fluids and fluid mixtures, *Fluid Phase Equilibria* **14**, 19 (1983).
- [37] R. F. Chang and J. M. H. L. Sengers, Behavior of dilute mixtures near the solvent’s critical point, *The Journal of Physical Chemistry* **90**, 5921 (1986), <https://doi.org/10.1021/j100280a093>.
- [38] Z. Ludmer, R. Shinnar, and V. Yakhot, Solubility in binary mixtures at the immiscibility critical point, *AIChE Journal* **33**, 1776 (1987).
- [39] J. Jiang and J. M. Prausnitz, Critical temperatures and pressures for hydrocarbon mixtures from an equation of state with renormalization-group theory corrections, *Fluid Phase Equilibria* **169**, 127 (2000).
- [40] J. Pérez-Pellitero, P. Ungerer, G. Orkoulas, and A. D. Mackie, Critical point estimation of the lennard-jones pure fluid and binary mixtures, *The Journal of Chemical Physics* **125**, 054515 (2006), <https://doi.org/10.1063/1.2227027>.
- [41] S. Artemenko, T. Lozovsky, and V. Mazur, Critical lines in binary mixtures of components with multiple critical points, in *Metastable Systems under Pressure*, edited by

- S. Rzoska, A. Drozd-Rzoska, and V. Mazur (Springer Netherlands, Dordrecht, 2010) pp. 217–232.
- [42] T. Yamamoto and M. Matsumoto, Solute effects on supercritical fluid, *Molecular Simulation* **37**, 1091 (2011), <https://doi.org/10.1080/08927022.2011.582104>.
- [43] I. H. Bell and A. Jäger, Calculation of critical points from helmholtz-energy-explicit mixture models, *Fluid Phase Equilibria* **433**, 159 (2017).
- [44] K. R. Harris and P. J. Newitt, Diffusion and structure in dilute aqueous alcohol solutions: Evidence for the effects of large apolar solutes on water, *The Journal of Physical Chemistry B* **102**, 8874 (1998).
- [45] H. S. Ashbaugh and M. E. Paulaitis, Effect of solute size and solute-water attractive interactions on hydration water structure around hydrophobic solutes, *Journal of the American Chemical Society* **123**, 10721 (2001), pMID: 11674005.
- [46] S. Chowdhuri and A. Chandra, Solute size effects on the solvation structure and diffusion of ions in liquid methanol under normal and cold conditions, *The Journal of Chemical Physics* **124**, 084507 (2006), <https://doi.org/10.1063/1.2172598>.
- [47] R. Okamoto and A. Onuki, Theory of nonionic hydrophobic solutes in mixture solvent: Solvent-mediated interaction and solute-induced phase separation, *The Journal of Chemical Physics* **149**, 014501 (2018), <https://doi.org/10.1063/1.5037673>.
- [48] A. Gao, R. C. Remsing, and J. D. Weeks, Short solvent model for ion correlations and hydrophobic association, *Proceedings of the National Academy of Sciences* **117**, 1293 (2020), <https://www.pnas.org/content/117/3/1293.full.pdf>.
- [49] E. A. Jagla, Phase behavior of a system of particles with core collapse, *Phys. Rev. E* **58**, 1478 (1998).
- [50] E. A. Jagla, Core-softened potentials and the anomalous properties of water, *The Journal of Chemical Physics* **111**, 8980 (1999), <https://doi.org/10.1063/1.480241>.
- [51] A. Oliveira, P. Netz, and M. Barbosa, Which mechanism underlies the water-like anomalies in core-softened potentials?, *The European Physical Journal B* **64**, 481 (2008).
- [52] M. Meyer and H. E. Stanley, Liquid-liquid phase transition in confined water: A monte carlo study, *The Journal of Physical Chemistry B* **103**, 9728 (1999), <https://doi.org/10.1021/jp984142f>.
- [53] L. B. Krott, J. R. Bordin, N. M. Barraza, and M. C. Barbosa, Effects of confinement on anomalies and phase transitions of core-softened fluids, *The Journal of Chemical Physics* **142**, 134502 (2015), <https://doi.org/10.1063/1.4916563>.
- [54] J. Bordin and M. Barbosa, Flow and structure of fluids in functionalized nanopores, *Physica A: Statistical Mechanics and its Applications* **467** (2016).
- [55] M. S. Marques, V. F. Hernandez, E. Lomba, and J. R. Bordin, Competing interactions near the liquid-liquid phase transition of core-softened water/methanol mixtures, *Journal of Molecular Liquids* **320**, 114420 (2020).
- [56] G. Munaò and T. Urbic, Structure and thermodynamics of core-softened models for alcohols, *The Journal of Chemical Physics* **142**, 214508 (2015), <https://doi.org/10.1063/1.4922164>.
- [57] G. Franzese, Differences between discontinuous and continuous soft-core attractive potentials: The appearance of density anomaly, *Journal of Molecular Liquids* **136**, 267 (2007), eMLG/JMLG 2006.
- [58] A. B. de Oliveira, G. Franzese, P. A. Netz, and M. C. Barbosa, Waterlike hierarchy of anomalies in a continuous spherical shouldered potential, *The Journal of Chemical Physics* **128**, 064901 (2008), <https://doi.org/10.1063/1.2830706>.
- [59] P. Vilaseca and G. Franzese, Softness dependence of the anomalies for the continuous shouldered well potential, *The Journal of Chemical Physics* **133**, 084507 (2010), <https://doi.org/10.1063/1.3463424>.
- [60] P. Vilaseca and G. Franzese, Isotropic soft-core potentials with two characteristic length scales and anomalous behaviour, *Journal of Non-Crystalline Solids* **357**, 419 (2011).
- [61] A. Kolb and B. Dünweg, Optimized constant pressure stochastic dynamics, *The Journal of Chemical Physics* **111**, 4453 (1999), <https://doi.org/10.1063/1.479208>.
- [62] H. Limbach, A. Arnold, B. Mann, and C. Holm, Espresso—an extensible simulation package for research on soft matter systems, *Computer Physics Communications* **174**, 704 (2006).
- [63] A. Arnold, O. Lenz, S. Kesselheim, R. Weeber, F. Fahrenberger, D. Roehm, P. Košovan, and C. Holm, Espresso 3.1: Molecular dynamics software for coarse-grained models, in *Meshfree Methods for Partial Differential Equations VI*, edited by M. Griebel and M. A. Schweitzer (Springer Berlin Heidelberg, Berlin, Heidelberg, 2013) pp. 1–23.
- [64] M. Allen, D. Tildesley, and D. Tildesley, *Computer Simulation of Liquids* (Oxford University Press, 2017).
- [65] M. Tuckerman, *Statistical Mechanics: Theory and Molecular Simulation*, Oxford graduate texts (Oxford University Press, 2010).
- [66] M. Dzugutov, Universal scaling law for atomic diffusion in condensed matter, *Nature* **381**, 137 (1996).
- [67] J. C. Dyre, Perspective: Excess-entropy scaling, *The Journal of Chemical Physics* **149**, 210901 (2018), <https://doi.org/10.1063/1.5055064>.
- [68] I. Bell, J. Dyre, and T. Ingebrigtsen, Excess-entropy scaling in supercooled binary mixtures, *Nature Communications* **2020**, 015012 (2020).
- [69] G. Galliero, C. Boned, and J. Fernández, Scaling of the viscosity of the lennard-jones chain fluid model, argon, and some normal alkanes, *The Journal of Chemical Physics* **134**, 064505 (2011), <https://doi.org/10.1063/1.3553262>.
- [70] H. J. Raveché, Entropy and molecular correlation functions in open systems. i. derivation, *The Journal of Chemical Physics* **55**, 2242 (1971), <https://doi.org/10.1063/1.1676399>.
- [71] A. Baranyai and D. J. Evans, Direct entropy calculation from computer simulation of liquids, *Phys. Rev. A* **40**, 3817 (1989).
- [72] R. Sharma, S. N. Chakraborty, and C. Chakravarty, Entropy, diffusivity, and structural order in liquids with waterlike anomalies, *The Journal of Chemical Physics* **125**, 204501 (2006), <https://doi.org/10.1063/1.2390710>.
- [73] J. R. Errington and P. D. Debenedetti, Relationship between structural order and the anomalies of liquid water, *Nature (London)* **409**, 318 (2001).
- [74] P. J. Steinhardt, D. R. Nelson, and M. Ronchetti, Bond-orientational order in liquids and glasses, *Phys. Rev. B* **28**, 784 (1983).
- [75] A. B. de Oliveira, P. A. Netz, T. Colla, and M. C. Barbosa, Structural anomalies for a three dimensional

- isotropic core-softened potential, *The Journal of Chemical Physics* **125**, 124503 (2006).
- [76] Z. Yan, S. V. Buldyrev, N. Giovambattista, and H. E. Stanley, Structural order for one-scale and two-scale potentials, *Phys. Rev. Lett.* **95**, 130604 (2005).
- [77] V. Ramasubramani, B. D. Dice, E. S. Harper, M. P. Spellings, J. A. Anderson, and S. C. Glotzer, *freud*: A software suite for high throughput analysis of particle simulation data, *Computer Physics Communications* **254**, 107275 (2020).
- [78] C. H. Rycroft, *Voro++*: A three-dimensional voronoi cell library in c++, *Chaos: An Interdisciplinary Journal of Nonlinear Science* **19**, 041111 (2009), <https://doi.org/10.1063/1.3215722>.
- [79] P. M. Larsen, S. Schmidt, and J. Schiøtz, Robust structural identification via polyhedral template matching, *Modelling and Simulation in Materials Science and Engineering* **24**, 055007 (2016).
- [80] A. Stukowski, Visualization and analysis of atomistic simulation data with OVITO - the Open Visualization Tool, *Modelling and Simulation in Materials Science and Engineering* **18**, 015012 (2010).
- [81] Stanley, H. E., Kumar, P., Franzese, G., Xu, L., Yan, Z., Mazza, M. G., Buldyrev, S. V., Chen, S.-H., and Mallamace, F., Liquid polyamorphism: Possible relation to the anomalous behaviour of water, *Eur. Phys. J. Special Topics* **161**, 1 (2008).
- [82] F. Mallamace, G. Mensitieri, D. Mallamace, M. Salzano de Luna, and S.-H. Chen, Some aspects of the liquid water thermodynamic behavior: From the stable to the deep supercooled regime, *International Journal of Molecular Sciences* **21**, 7269 (2020).
- [83] D. Corradini, S. V. Buldyrev, P. Gallo, and H. E. Stanley, Effect of hydrophobic solutes on the liquid-liquid critical point, *Phys. Rev. E* **81**, 061504 (2010).
- [84] M. Huš and T. Urbic, Core-softened fluids as a model for water and the hydrophobic effect, *The Journal of Chemical Physics* **139**, 114504 (2013), <https://doi.org/10.1063/1.4821226>.
- [85] M. Hus and T. Urbic, Existence of a liquid-liquid phase transition in methanol, *Phys. Rev. E* **90**, 062306 (2014).
- [86] G. Wada and S. Umeda, Effects of nonelectrolytes on the temperature of the maximum density of water. i. alcohols, *Bulletin of the Chemical Society of Japan* **35**, 646 (1962), <https://doi.org/10.1246/bcsj.35.646>.
- [87] D. González-Salgado, J. Troncoso, and E. Lomba, The temperature of maximum density for amino acid aqueous solutions. an experimental and molecular dynamics study, *Fluid Phase Equilibria*, 112703 (2020).
- [88] E. Salcedo, N. M. Barraz, and M. C. Barbosa, Relation between occupation in the first coordination shells and widom line in core-softened potentials, *The Journal of Chemical Physics* **138**, 164502 (2013), <https://doi.org/10.1063/1.4802006>.
- [89] M. S. Marques, T. P. O. Nogueira, R. F. Dillenburg, M. C. Barbosa, and J. R. Bordin, Waterlike anomalies in hard core-soft shell nanoparticles using an effective potential approach: Pinned vs adsorbed polymers, *Journal of Applied Physics* **127**, 054701 (2020), <https://doi.org/10.1063/1.5128938>.
- [90] F. Mallamace, The liquid water polymorphism, *Proceedings of the National Academy of Sciences* **106**, 15097 (2009), <https://www.pnas.org/content/106/36/15097.full.pdf>.